Proximity of Cytoplasmic and Periplasmic Loops in NhaA Na^+/H^+ Antiporter of *Escherichia coli* As Determined by Site-Directed Thiol Cross-Linking†

A. Rimon, T. Tzubery, L. Galili, and E. Padan*

Alexander Silberman Institute of Life Sciences, Hebrew University of Jerusalem, 91904 Jerusalem, Israel

Received May 15, 2002; Revised Manuscript Received June 26, 2002

ABSTRACT: The unique trypsin cleavable site of NhaA, the Na^+/H^+ antiporter of *Escherichia coli*, was exploited to detect a change in mobility of cross-linked products of NhaA by polyacrylamide gel electrophoresis. Double-Cys replacements were introduced into loops, one on each side of the trypsin cleavage site (Lys 249). The proximity of paired Cys residues was assessed by disulfide cross-linking of the two tryptic fragments, using three homobifunctional cross-linking agents: 1,6-bis(maleimido)hexane (BMH), *N*,*N*′-*o*-phenylenedimaleimide (*o*-PDM), and *N*,*N*′-*p*-phenylenedimaleimide (*p*-PDM). The interloop cross-linking was found to be very specific, indicating that the loops are not merely random coils that interact randomly. In the periplasmic side of NhaA, two patterns of cross-linking are observed: (a) all three cross-linking reagents cross-link very efficiently between the double-Cys replacements A118C/S286C, N177C/S352C, and H225C/S352C; (b) only BMH cross-links the double-Cys replacements A118C/S352C, N177C/S286C, and H225C/S286C. In the cytoplasmic side of NhaA, three patterns of cross-linking are observed: (a) all three cross-linking reagents cross-link very efficiently the pairs of Cys replacements L4C/E252C, S146C/L316C, S146C/R383C, and E241C/E252C; (b) BMH and *p*-PDM cross-link efficiently the pairs of Cys replacements S87C/E252C, S87C/L316C, and S146C/E252C; (c) none of the reagents cross-links the double-Cys replacements L4C/L316C, L4C/R383C, S87C/R383C, A202C/E252C, A202C/L316C, A202C/R383C, E241C/L316C, and E241C/R383C. The data reveal that the N-terminus and loop VIII−IX that have previously been shown to change conformation with pH are in close proximity within the NhaA protein. The data also suggest close proximity between N-terminal and C-terminal helices at both the cytoplasmic and the periplasmic face of NhaA.

Sodium proton antiporters are ubiquitous membrane proteins found in the cytoplasmic and organelle membranes of cells of many different origins, including plants, animals, and microorganisms. They are involved in cell energetics, and play primary roles in the regulation of intracellular pH, cellular Na^+ content, and cell volume [reviewed in (*1*−*4*)].

Escherichia coli has two Na^+ (and Li^+) specific Na^+/H^+ antiporters encoded by *nha*A and *nha*B (*4*−*6*). NhaA is the essential Na^+/H^+ antiporter for $H^+$and Na^+ homeostasis in *E. coli* (*1*−*3, 5*). The expression of *nha*A is positively regulated by NhaR, a member of the LysR family, and is induced by Na^+ in a pH-dependent manner [reviewed in (*2*)].

NhaA is an electrogenic antiporter that has been purified to homogeneity and reconstituted in a functional form in proteoliposomes (*7*). The H^+/Na^+ stoichiometry of NhaA is $2H^+/Na^+$ (*8*). The activity of NhaA is highly dependent on pH, with the V_{max} changing by over 3 orders of magnitude from pH 7 to 8.5 (*7, 9*). Several amino acids (*9*−*12*) and pH-induced conformational changes (*13, 14*) are involved in the pH regulation of NhaA. The conformational changes involve loop VIII−IX (*13*) and the N-terminus of NhaA (*14*).

The NhaA protein is predicted to have a putative secondary structure consisting of 12 TMS[1] connected by hydrophilic loops (*15*). This predicted topology has been substantiated by using *pho*A fusions combined with epitope mapping, exposure to proteolysis, and accessibility of site-directed Cys replacements from each side of the membrane (*15, 16*).

NhaA, as for any other of the secondary transporters, has not yet been solved at atomic resolution. However, recently 2D crystals of NhaA diffracting at 4 Å were obtained. Cryo-electron microscopy of these crystals showed that NhaA exists as a dimer of monomers composed of 12 helices (*17*). In the native membrane, NhaA forms oligomers within which the monomers physically and functionally interact (*18*). The 2D crystals also produced a three-dimensional map of NhaA (*19*), the first insight into the architecture of the helices of the protein.

† This research was supported first by a grant from the GIF, the German−Israeli Foundation for Scientific Research and Development (to E.P.), and then by the BMBF and the International Bureau of the BMBF at the DLR [German−Israeli Project Cooperation on Future Oriented Topics (DIP) (to E.P.)] and the Israel Science Foundation. The Moshe Shilo Minerva Center for Biogeochemistry is also acknowledged. E.P. was awarded the Massimo and Adelina Della Pergolla Chair in Life Sciences.

* Correspondence should be addressed to this author. Tel: 972-2-6585094. Fax: 972-2-6586947. Email: etana@vms.huji.ac.il.

[1] Abbreviations: TMS, transmembrane segment; BTP, 1,3-bis[[tris(hydroxymethyl)methyl]amino]propane; ΔpH, pH difference across the membrane; TCA, trichloroacetic acid; Ni-NTA, Ni^{2+} nitrilotriacetic acid; DTT, dithiothreitol; BMH, 1,6-bis(maleimido)hexane; *o*-PDM, *N*,*N*′-*o*-phenylenedimaleimide; *p*-PDM, *N*,*N*′-*p*-phenylenedimaleimide; MOPS, 3-(*N*-morpholino)propanesulfonic acid; DM, *n*-dodecyl-*β*-D-maltoside; HEPES, *N*-(2-hydroxyethyl)piperazine-*N*′-2-ethanesulfonic acid; PAGE, polyacrylamide gel electrophoresis; H4C, NhaA-His 4 replaced with Cys, all other *nha*A mutations are accordingly depicted; KPi, potassium phosphate.

10.1021/bi0261342 CCC: $22.00
Published on Web 11/20/2002

Table 1: Primers Used for Construction of NhaA Mutants

mutation	DNA sequence of mutagenetic oligonucleotide[a]	codon change observed	new restriction site
L4C	GTGAAACATTGTCACCGGTTC	CTG → TGT	*Age*I
A118C	GCTTTTAACTATTGTGACCCGATTACC	GCC → TGT	*Tsp*45I
S146C	GCTGTTGGGCTGCAGAGTTCCGTTAGC	AGT → TGC	*Pst*I
N177C	GCATTGTTCTACACGTGTGACTTATCG	AAT → TGT	*Pml*I
A202C	GTCTGGTTGTCGACGCACGGGCG	GCA → TGT	*Sal*I
E252C	GCGACTGTGTCACGTGTTGCACCC	GAG → TGT	*Eco*72I
S286C	GCTTGACATGCATTCTGCCATTGG	TCC → TGC	*Mph*1103I
A248	GTTCTCCAGCCAAGCGACTGGAGCATGTG	GCG → GCC	*Bst*XI

[a] The changed bases are underlined.

Site-directed thiol cross-linking has been used to determine interhelical and interloop interaction in many membrane proteins (*20*−*22*). In this approach, a pair of Cys replacements are introduced into the protein. Then thiol cross-linking reagents of various distances between the reactive groups are applied on the membrane, and the degree of cross-linking in the protein is assessed. In this study, we have used this approach in situ (*21, 22*) to determine the proximity between pairs of Cys replacements in cytoplasmic and periplasmic loops of NhaA. The interloop cross-linking was found to be very specific and revealed that the N-terminus and loop VIII−IX, that have previously been shown to change conformation with pH, are in close proximity within the NhaA protein. The data also suggest close proximity between N-terminal and C-terminal helices, both at the cytoplasmic and at the periplasmic face of NhaA.

EXPERIMENTAL PROCEDURES

Bacterial Strains and Culture Conditions. EP432 is an *E. coli* K12 derivative, which is *mel*BLid, Δ*nha*A1::*kan*, Δ*nha*B1::*cat*, Δ*lac*ZY, *thr*1 (*6*). TA16 is *nha*A$^+$*nha*B$^+$*lac*I^Q and otherwise isogenic to EP432 (*7*). DH5α (United States Biochemical Corp.) was used as a host for construction of plasmids. Cells were grown in modified L broth (LBK) in which NaCl was replaced by KCl (87 mM, pH 7.5). The medium was buffered by 60 mM BTP, and the pH was titrated with HCl. Cells were also grown in minimal medium A without sodium citrate (*23*) with glycerol (0.5%) as a carbon source. Thiamin (2.5 μg/mL) was added to all minimal media. For EP432, threonine (0.1 mg/mL) was also added; for plates, 1.5% agar was used. The antibiotics and their concentrations were 100 μg/mL ampicillin and 50 μg/mL kanamycin. Resistance to Li^+ and Na^+ was tested as described previously (*5*).

Plasmids. All plasmids used here encode NhaA lacking its native cysteines (C-less, CL). pC-less-XH2 was previously described (*18*). pCLHAH3 is a plasmid encoding a modified NhaA in which the native C-terminal sequence from R383 to V388 was replaced with R381V382AYPYDVPDYALEHHHHHH, a hemagglutinine epitope allowed by six His (His-tag). This plasmid was obtained by digestion of pC-less-XH2 with *Mlu*I and *Xho*I and ligating the fragment (4708 kb) with the linker: CGCGTGGCCTACCCATATGACGTGCCCGATTATGCTC. pCLHAH4 is identical with pCLHAH3 but contains a silent mutation that introduced *Bst*XI at codon 248 (Table 1). PClHAH2 is a plasmid encoding a modified NhaA in which the native C-terminal sequence from R383 to V388 was replaced with the linker CGCGCGTGCTACCCATATGACGTGCCCGATTATGCTC as described above and contains a Cys at 383. These three versions of NhaA have a wild-type phenotype with respect to supporting growth of EP432, expression in the membrane, and Na^+/H^+ antiporter activity (data not shown). In addition, similar to the wild-type NhaA, they all have at alkaline pH only one trypsin cleavable site at K249.

Site-Directed Mutagenesis. Site-directed mutagenesis was conducted following a polymerase chain reaction-based protocol (*24*). The mutagenic primers used are described in Table 1.

Single-Cys Mutants. The single-Cys mutants encoded by C-less pAXH2 and previously described (*18*) were S52C, S87C, H225C, E241C, L316C, and S352C using the mutagenic primers described in Table 1. The mutants L4C, A118C, S146C, N177C, A202C, and S286C were constructed on plasmid pCLHAH4 and E252C on plasmid pCLHAH3. All plasmidic single NhaA mutants were transformed into EP432 for phenotype analysis. They were all expressed (50−100% of the wild-type), support growth of EP432 in 0.6 M NaCl both at pH 7 and at pH 8.3, and exhibit Na^+/H^+ antiporter activity in isolated membrane vesicles (50−100% of the wild-type activity) (data not shown).

Double-Cys Mutants. Using the plasmid encoding single-Cys NhaA mutants, the given double-Cys mutants were generated by restriction fragment replacement. Mutations were verified by DNA sequencing.

Isolation of Membrane Vesicles, Assay of Na^+/H^+ Antiporter Activity. Assays of Na^+/H^+ antiport activity were conducted on everted membrane vesicles of EP432 (*25, 26*). A fluorescence assay of antiport activity was performed as described (*26*) using acridine orange to measure generation of ΔpH. After energization with Tris−D-lactate or ATP (2 mM each), quenching of the fluorescence was allowed to achieve a steady state, and then either Na^+ or Li^+ was added. A reversal quenching (dequenching) indicates that H^+ is exiting the vesicle in antiport with the indicated cation. The reaction mixture contained 50−100 μg of membrane protein, 0.5 μM acridine orange, 140 mM KCl, 50 mM BTP, and 5 mM $MgCl_2$, and the pH was titrated with HCl.

Overexpression and Affinity Purification of His-Tagged Antiporters by Ni^{2+}-NTA Chromatography. To overexpress the plasmids encoding the His-tagged antiporters, TA16 transformed with the respective plasmids were used as described (*7*), and high-pressure membranes were prepared as described (*7*).

His-tagged NhaA was affinity-purified on Ni-NTA-agarose resin (Qiagen, Hilden, Germany) by miniscale purification and eluted with imidazole, as described (*16, 27*). The protein was precipitated in 10% TCA for 0.5 h at 4 °C, centrifuged

(14 000 rpm, 30 min at 4 °C) and resuspended in sampling buffer, titrated to neutrality with Tris base, and loaded on the gel for SDS−PAGE as described (*28*).

Protein Determination. Protein was determined according to (*29*).

DNA Sequence. Sequencing of DNA was conducted by an automated DNA sequencer (ABI PRISM 377, Perkin-Elmer).

Detection and Quantitation of NhaA and Its Mutated Proteins in the Membrane. Detection and quantitation of NhaA and its mutated derivatives in membranes of EP432 were conducted by Western analysis as described previously (*9*). The antibodies used were mAb 1F6 (*30*). The amount of affinity-purified NhaA and its mutants was determined by Coomassie staining of the gel after SDS−PAGE and scanning as described previously (*18, 28*).

In Situ Site-Directed Cross-Linking. High-pressure membranes (*7*) were prepared from TA16 cells transformed with each one of the plasmids encoding the double-Cys mutations. Membranes (3 mg of protein) were resuspended in a buffer (4.5 mL) containing 100 mM KPi, 5 mM $MgSO_4$ (pH 7.3), and one of the homobifunctional cross-linkers was added [BMH (Pierce), 2 mM, or *o*-PDM (Sigma) or *p*-PDM (Sigma) (1 mM each)]. The suspension was incubated at 25 °C with gentle rotation for 60 min. The reaction was terminated by the addition of 10 mM DTT. The membranes were washed in 3 mL containing 140 mM choline chloride, 250 mM sucrose, and 10 mM Tris-HCl (pH 7) and resuspended in 1.15 mL of the same solution but containing in addition 20% glycerol, 1% DM, and 0.1 M MOPS (pH 7). The suspension was incubated with gentle tilting for 30 min at 4 °C and centrifuged (20 min, 75 000 rpm, Beckman, TLA), and the supernatant was incubated with 250 μL of Ni^{2+}-NTA-agarose (Qiagene) for miniscale purification of NhaA as described above. For trypsin treatment, 15 μg of protein was resuspended in 0.5 mL containing 0.1 M KCl, 0.7 mM EDTA, 1 mM $CaCl_2$, 0.1% DM, and 50 mM Tris/HEPES (pH 8.5), 300 ng of trypsin (Sigma type III) was added, and the suspension was incubated at 37 °C for 1 h. The reaction was terminated by 900 ng of trypsin inhibitor type II (Sigma); then the protein was precipitated by incubation for 30 min at 4 °C in the presence of 10% TCA and resolved on SDS−PAGE as described (*18, 28*).

Accessibility of the Cys Replacements to the Cross-Linking Reagents. To determine the accessibility of the Cys replacements to the cross-linking reagents, membranes were treated in situ with the cross-linking reagents, the reaction was terminated by the addition of β-mercaptoethanol, and the membranes were processed as described above. Following the addition of the trypsin inhibitor, 0.2 mM fluorescein-5-maleimide (Molecular Probes) was added. The suspension was incubated with gentle tilting for 30 min at 25 °C, and the reaction was terminated by the addition of 2 mM β-mercaptoethanol. For evaluation of the fluorescence labeling, dried SDS−PAGE gels were photographed under UV light (260 nm).

RESULTS

Construction of Pairs of Cys Replacements in the Loops of NhaA. In this study, the distances between loops (cytoplasmic or periplasmic) of NhaA were determined by site-directed thiol cross-linking between the loops. For this purpose, we used plasmids encoding Cys-less His-tagged NhaA to construct NhaA mutants containing each double-Cys replacements, one replacement per loop (Table 2 and Figure 1).

Table 2: Double-Cys Replacements in NhaA Loops

mutations[a]	expression, % of total membrane protein[b]	growth in 0.6 M NaCl		activity, % dequenching at pH 8.5[c]
		pH 7	pH 8.3	
Periplasmic Loops				
A118C/S286C***	1.2	+	+	50
A118C/S352C***	1.1	+	+	49
N177C/S286C***	1.3	+	+	51
N177C/S252C***	1.3	+	+	50
H225C/S286C***	3	+	+	30
H225C/S352C**	3.1	+	+	23
Cytoplasmic Loops				
L4C/E252C	0.7	+	+	28
L4C/L316C***	0.8	+	+	28
L4C/383C*	0.8	+	+	50
S87C/E252C**	0.7	+	+	29
S87C/L316C***	0.8	+	+	30
S87C/383C*	0.8	+	+	50
S146C/E252C**	0.9	+	+	18
S146C/L316C***	0.8	+	+	45
S146C/383C*	0.8	+	+	44
A202C/E252C**	2.3	+	+	77
A202C/L316C***	2.9	+	+	78
A202C/383C*	2.7	+	+	82
E241C/E252C**	2.4	+	+	56
E241C/L316C***	3.4	+	+	64
E241C/383C*	3.5	+	+	88
pBR322		−	−	0
pCLHAH4	3.4	+	+	80

[a] Mutations expressed by the letter code of amino acids: first, the wild-type, followed by the codon number, then the replacement. The mutation L4C/E252C was constructed in plasmid parent pCLAXH2. The other mutations were constructed in pCLHAH2*, or pCLHAH3**, or pCLHAH4***. [b] TA16 cells transformed with the indicated plasmids were grown in medium A, high-pressure membranes were prepared, His-tagged NhaA was purified on Ni-NTA-agarose, and protein was determined as described under Experimental Procedures. [c] Assay of the Na^+/H^+ antiporter activity was conducted on everted membrane vesicles isolated from EP432 cells transformed with the indicated plasmids. EP432/pCLHAH4 served as a positive control.

To determine the level of expression and phenotype of the mutants, the plasmidic mutants were transformed into EP432, an *E. coli* strain devoid of both Na^+-specific antiporters NhaA and NhaB (*5*). This strain can grow in the presence of high Na^+ or Li^+ only when transformed with a plasmid expressing active NhaA. The results summarized in Table 2 show that all double mutants are expressed to a level which is at least 20% of the wild-type level (EP432/pCLHAH4). It should be noted that these expression levels that are obtained from multicopy plasmids are way above the level observed in wild-type strains carrying a single copy of *nha*A (*11*). Indeed, all mutants grow on Na^+ both at neutral and at alkaline pH (Table 2).

To determine the Na^+/H^+ antiporter activity, everted membrane vesicles were isolated from each of the double mutants expressed in EP432 from the respective plasmids. The Na^+/H^+ antiporter activity was measured at pH 8.5 as recovery from the respiratory-dependent fluorescence quenching of acridine orange upon addition of Na^+. Membranes derived from EP432 cells transformed with the vector plasmid have no Na^+/H^+ antiporter activity [Table 2 and

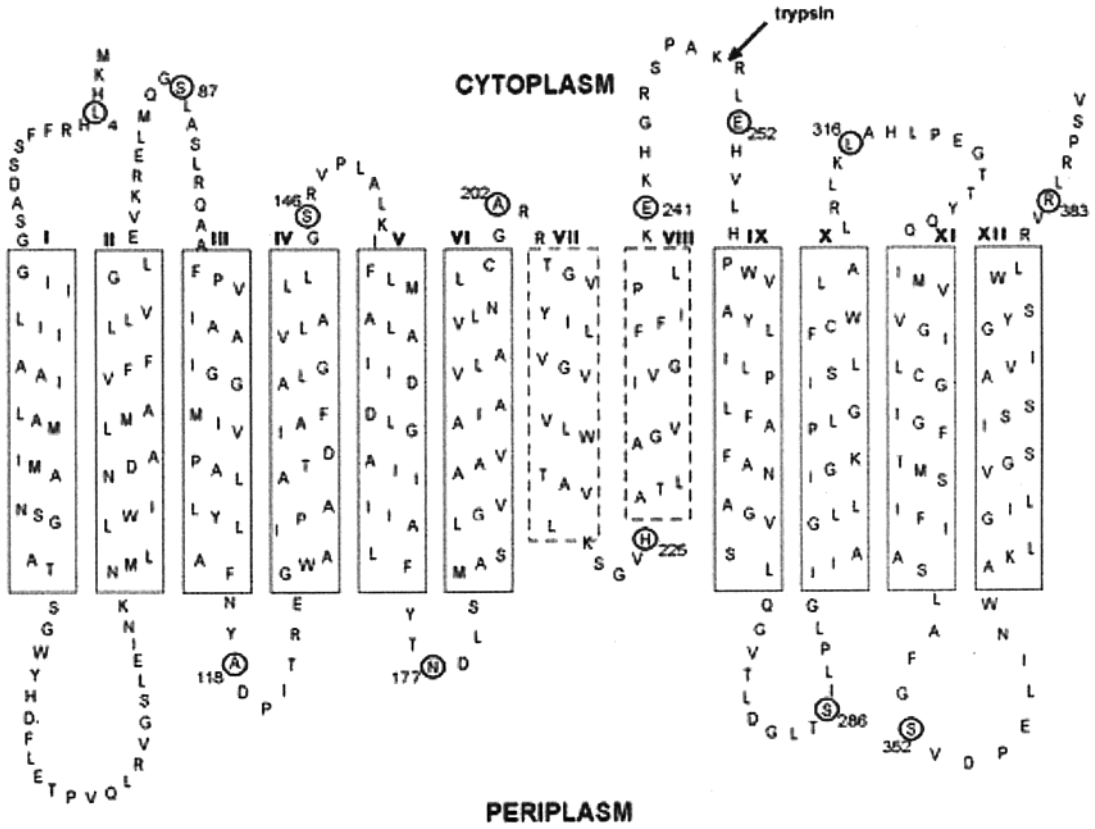

FIGURE 1: Secondary structure model of NhaA and Cys replacements in the loops. The 12 transmembrane segment model proposed for the topology of NhaA (*15*) is shown. The single-letter amino acid code is used, and the location in the amino acid sequence is indicated by a number. The Roman numerals indicate the number of the TMS. Residues that were replaced by Cys in this work are encircled.

(*6*)]. Transformation with the wild-type NhaA plasmid restores Na^+/H^+ antiporter activity [Table 2 and (*6*)]. The results show that all double mutants exhibit substantial Na^+/H^+ antiporter activity, varying between 20 and 100% of the wild-type activity (Table 2).

Developing a Protocol To Determine in Situ Cross-Linking between Loops of NhaA. For the chemical cross-linking experiments, membrane vesicles were isolated from cells expressing the mutated plasmids, and cross-linking agents were applied in situ on the membranes. Then the His-tagged proteins were affinity-purified, and the mobilities of the treated and nontreated proteins were compared by SDS−PAGE. Treatment with cross-linking agents did not alter the electrophoretic mobility of the proteins (data not shown). This negative result could be interpreted in two ways: The Cys replacements in the loops of NhaA are not exposed to the cross-linking agent; the cross-linked NhaA has a mobility identical to that for the non-cross-linked NhaA, a situation found in other prokaryotic membrane proteins (*22, 31*). Therefore, to apply the cross-linking approach, we first had to develop an assay to detect the cross-linked products of NhaA.

We have previously shown that NhaA has one trypsin cleavable site that becomes exposed at alkaline pH only (*13*). Following trypsin digestion at alkaline pH, NhaA is split at K249 in loop VIII−IX [Figures 1 and 2 and (*13*)]. The resulting two polypeptides can easily be identified by SDS−PAGE as 24 and 17 kDa fragments [Figure 2A, lane 3 and (*13*)] with intact NhaA bands at 32.5 kDa [Figure 2A, lane 2 and (*13*)]. Note that the size of both His-tagged NhaA and its tryptic products have lower apparent size in SDS−PAGE than the molecular masses calculated from their deduced amino acid sequence, i.e., 43.5, 26.4, and 17.1 kDa, respectively (*13*). This aberrant mobility in SDS−PAGE is characteristic of many integral polytopic membrane proteins (*7, 13*). Based on these findings, we developed an assay to identify intramolecular cross-linking of NhaA. For this purpose, we constructed the double-Cys replacement mutants of NhaA so that the two NhaA fragments obtained following trypsin digestion at alkaline pH each contain one Cys replacement (Table 2 and Figure 1). Given that cross-linking occurs between these Cys residues, following trypsin digestion, only one fragment of a size identical with NhaA monomer is expected. In contrast, two fragments are expected from both the untreated control as well as the non-cross-linked double-Cys mutants.

The protocol is exemplified with the double-Cys mutant A118C/S286C (Figure 2A). Membranes expressing this mutant were treated in situ with three different homobifunctional cross-linking agents in which the distance between the reactive groups and the resiliency of the linker between the functional groups vary: BMH is the most resilient whereas *o*-PDM and *p*-PDM are not. The range of distances between the double-Cys replacements required for cross-linking by these reagents is 3.5−15.6, 7.7−10.5, and 9.2−12.3 Å, respectively (*32*). The protein was then affinity-purified and subjected to digestion with trypsin at alkaline pH, and the products were resolved on SDS−PAGE. For control, membranes expressing the A118C/S286C mutant were treated in the same way but without addition of the cross-linking agents (Figure 2A, lane 2). The results clearly show that following BMH treatment, only one band similar

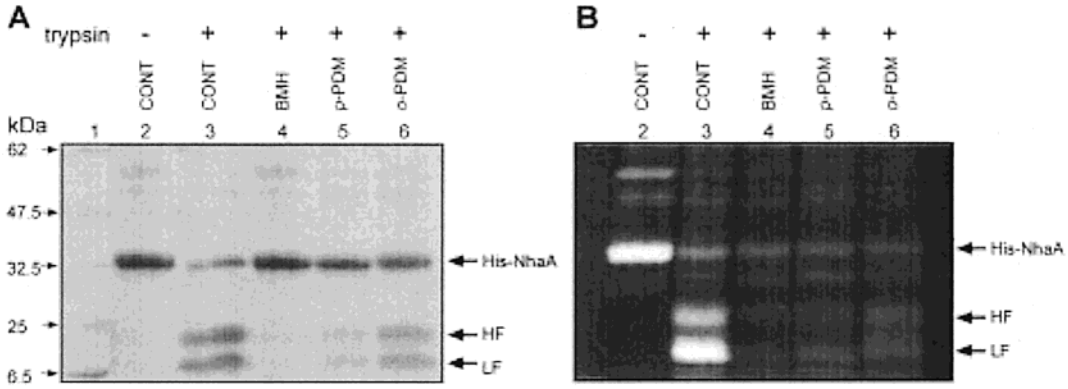

FIGURE 2: Analysis of in situ intramolecular cross-linking between A118C of loop III−IV and S286C of loop IX−X of NhaA. (A) Membrane vesicles (3 mg of protein) prepared from TA16/pA118C/S286C cells were subjected in situ to the cross-linking agents. Then the His-tagged double mutant NhaA was affinity-purified, subjected to digestion by trypsin, resolved on SDS−PAGE, and Coomassie-stained. The mobility of the intact His-tagged NhaA and the tryptic fragments of NhaA, HF (heavy fragment) and LF (light fragment), are indicated. For details of all steps, see Experimental Procedures. (B) Membrane vesicles were treated with cross-linking agents and processed as in panel A except for the fluorescein maleimide (0.2 mM) that was added following trypsin treatment. The gels were photographed by a UV camera.

Table 3: Homobifunctional Cross-Linking of Double-Cys Replacement Mutants in Loops of NhaA[a]

mutants	loops	BMH 10.2 ± 2.4 Å	*p*-PDM 11.1 ± 0.5 Å	*o*-PDM 9.4 ± 0.5 Å
	Periplasmic			
A118C/S286C	III−IV/IX−X	+	+	+
A118C/S352C	III−IV/XI−XII	+	−	−
N177C/S286C	V−VI/IX−X	+	−	−
N177C/S352C	V−VI/XI−XII	+	+	+
H225C/S286C	VII−VIII/IX−X	+	−	−
H225C/S352C	VII−VIII/XI−XII	+	+	+
	Cytoplasmic			
L4C/E252C	I/VIII−IX	+	+	+
L4C/L316C	I/X−XI	−	−	−
L4C/R383C	I/XII	−	−	−
S87C/E252C	II−III/VIII−IX	+	+	−
S87C/L316C	II−III/X−XI	+	+	−
S87C/R383C	II−III/XII	−	−	−
S146C/E252C	IV−V/VIII−IX	+	+	−
S146C/L316C	IV−V/X−XI	+	+	+
S146C/R383C	IV−V/XII	+	+	+
A202C/E252C	VI−VII/VIII−IX	−	−	−
A202C/L316C	VI−VII/X−XI	−	−	−
A202C/R383C	VI−VII/XII	−	−	−
E241C/E252C	VIII−IX/VIII−IX	+	+	+
E241C/L316C	VIII−IX/X−XI	−	−	−
E241C/R383C	VIII−IX/XII	−	−	−

[a] A summary of the cross-linking results is presented in Figures 3 and 4. +, positive cross-linking; −, no cross-linking. The average span widths of the various cross-linking agents are taken from (*32*).

in size to uncut NhaA (32.5 kDa) was obtained (Figure 2A, lane 4) as opposed to the two fragments produced without the addition of the cross-linking agent (Figure 2A, lane 3). When DTT (10 mM) was added together with the cross-linkers or when Cys-less NhaA was used, no cross-linked tryptic fragments of NhaA were observed (data not shown). These results show that the double-Cys replacements, A118C in loop III−IV and S286 in loop IX−X, are cross-linked by BMH. Figure 2 also shows that the shorter the distance between the reactive groups of the cross-linking agent, the less cross-linking was obtained between loop III−IV and loop IX−X. Thus, following tryptic cleavage of *p*-PDM-treated membranes, the two tryptic peptides could be observed, but their concentration was very low (Figure 2A, lane 5). Following *o*-PDM treatment, the intensity of the tryptic peptides was about half of the control (Figure 2, lane 6). As previously shown (*13*), in most cases the tryptic fragments of NhaA at alkaline pH (LF and HF, Figure 2) were very stable and resistant to further digestion by trypsin. Therefore, for most cases, a decrease in the amount of the tryptic fragments correlated with an increase in the 32.5 kDa band (Figure 2A). As a routine, we scored as positive results a level of cross-linking that was above 50% (Table 3). Note that, for unknown reasons, a small fraction of NhaA was not digested by trypsin. However, this fraction had no effect on our way of evaluation since in each mutant the degree of cleavage without cross-linking was assessed and used as a reference point.

Since our assay for cross-linking is based on digestion by trypsin, it could be argued that the cross-linking itself interferes with the trypsin digestion and therefore only a single band, equal in size to the intact protein, was obtained. To test this possibility, the membranes expressing the mutated protein were first treated with trypsin and only then treated with the cross-linking agent. This approach could be applied since we had previously shown that both tryptic fragments of the trypsin-splitted NhaA protein were complexed to each other and co-purified via the His-tag at the C-terminus (*13*). Since the results obtained with the two procedures were identical (data not shown), we adopted the protocol described in Figure 2.

Accessibility of the Cross-Linking Agents. When cross-linking was partial (Figure 2A, lanes 5 and 6) or did not take place at all as, for example, with the double mutant A202C/R383C (Figure 4L), the results could be interpreted in two ways: (a) a large distance exists between the double-Cys residues so that the cross-linking molecule could not span the gap; (b) the cross-linking agents are not accessible or not reactive with the Cys replacements. To answer these questions, we determined the accessibility of the mutants to the cross-linking agents using fluorescein maleimide which links a fluorescent molecule to the Cys residues. Each protein fraction described in Figure 2A was treated with fluorescein maleimide before being applied to the gel, and then the SDS−PAGE was conducted. Figure 2B, lane 2, shows that the intact mutant protein was labeled by fluorescein maleimide. Since each Cys replacement of the mutant was introduced into the opposite sides of the trypsin cleavage

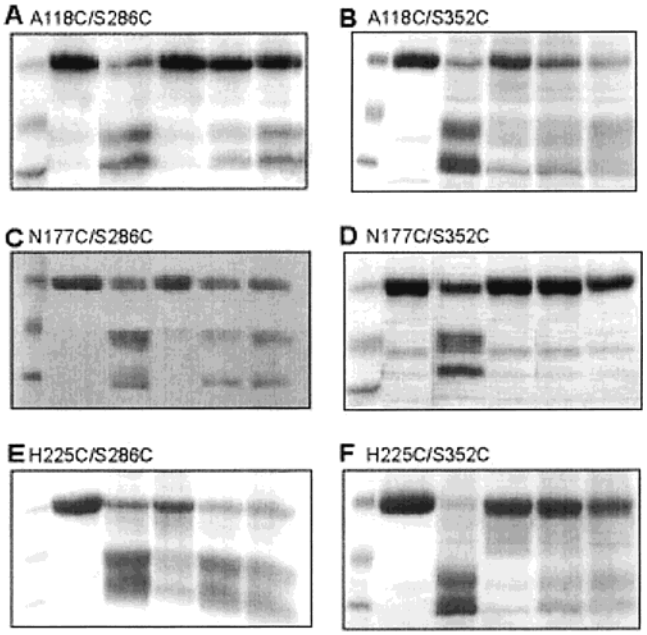

FIGURE 3: In situ cross-linking results between periplasmic loops of NhaA. The indicated double-Cys replacement mutants in the periplasmic loops of NhaA were cross-linked in situ by BMH (lanes 4), *p*-PDM (lanes 5), or *o*-PDM (lanes 6) or not cross-linked (lanes 3), treated with trypsin, and processed as described in Figure 2. Lane 2 in each case contained a control that was not treated with either cross-linker agent or trypsin. Lane 1 in each case contained molecular mass markers (32.5, 25, and 16.5 kDa). The presented results are representative of experiments performed twice or more.

site, both tryptic fragments of the mutant were also labeled by fluorescein maleimide (Figure 2B, lane 3). Pretreatment with any of the cross-linking agents drastically reduced the degree of fluorescent labeling of A118C/S286C (Figure 2B, lanes 4−6). These results show that the cross-linker reacted with the Cys replacements and competed with the fluorescent maleimide. We used this fluorescein assay to assess the accessibility and chemical reactivity of all cross-linking agents. All double-Cys replacements used here were found accessible to and reactive with all three cross-linking agents (data not shown). It should also be noted that fluorescein maleimide did not label a Cys-less NhaA (data not shown).

NhaA is an oligomer in the native membrane (*18*), and we have previously shown that V254C of loop VIII−IX and S52C of loop I−II undergo intermolecular cross-linking (*18*). Since intermolecular cross-linking can complicate the interpretation of the intramolecular cross-linking assay, we avoided the use of V254C and S52C. Furthermore, each of the single and double mutants was first tested for intermolecular cross-linking as described previously (*18*). None of the mutants used in the present work showed any intermolecular cross-linking.

Cross-Linking between Periplasmic Loops of NhaA. The periplasmic loops of NhaA are loops I−II, III−IV, V−VI, VII−VIII, IX−X, and XI−XII [Figure 1 and (*15*)]. The results shown in Figure 3 and Table 3 compile the cross-linking results between the periplasmic loops. Two patterns of cross-linking are observed: (a) all three cross-linking reagents cross-link very efficiently between the double-Cys replacements A118C/S286C, N177C/S352C, and H225C/S352C; (b) only BMH cross-links the double-Cys replacements A118C/S352C, N177C/S286C, and H225C/S286C.

Cross-Linking between Cytoplasmic Loops of NhaA. The N-terminus and the C-terminus of NhaA are cytoplasmic [Figure 1 and (*15*)]. The cytoplasmic loops of NhaA are loops II−III, IV−V, VI−VII, VIII−IX, and X−XI. The results shown in Figure 4 and Table 3 compile the cross-linking results between the cytoplasmic loops.

In the cytoplasmic side of NhaA, three patterns of cross-linking are observed: (a) all three cross-linking reagents cross-link very efficiently the pairs of Cys replacements L4C/E252C, S146C/L316C, S146C/R383C, and E241C/E252C; (b) BMH and *p*-PDM cross-link efficiently the pairs of Cys replacements S87C/E252C, S87C/L316C, and S146C/E252C; (c) none of the reagents cross-links the double-Cys replacements L4C/L316C, L4C/R383C, S87C/R383C, A202C/E252C, A202C/L316C, A202C/R383C, E241C/L316C, and E241C/R383C.

DISCUSSION

In this study, the unique trypsin cleavable site of NhaA at alkaline pH [K249 (*13*)] is exploited to detect a change in mobility in SDS−PAGE, of cross-linked products of NhaA. Double-Cys replacements were introduced into loops, one on the N-terminal side and the other on the C-terminal side of the cleavage site. Proximity of paired Cys residues was assessed by disulfide cross-linking of the two tryptic fragments (24 and 17 kDa) which when cross-linked acquire together a mobility in SDS−PAGE identical to that of intact NhaA (32.5 kDa).

This detection assay was found to be very reproducible. In most cases, when cross-linking occurred, a marked increase in the intensity of the 32.5 kDa band correlated with a decrease in the shorter tryptic fragments. Only in very few cases (see Figure 4A) did further proteolysis, mainly of the heavy tryptic fragment, occur. The light tryptic fragment was previously found to be more resistant to further proteolysis than the heavy fragment (*13*).

We chose to score as positive cross-linking only cases where less than 50% of the cleavage products were observed. In cases where partial cross-linking was observed, no attempt was made to improve the cross-linking by prolonging the incubation time, changing the pH, or increasing the concentration of the reagent. Therefore, our results can slightly underestimate the real cross-linking capabilities of the reagents, and, therefore, overestimate the distances between the respective residues.

Certain proteins, such as the metal-tetracycline/H^+ antiporter (*33*) when cross-linked within the molecule, have a mobility in SDS−PAGE which is markedly different from that of the un-cross-linked molecule. Presumably, this is due to two very different configurations before and after cross-linking. In the case of NhaA and similarly with both the Lac permease (*34*) as well as MelB (*31*), no perceptible changes in the apparent molecular weight of the proteins have been detected after treatment with cross-linking reagents. In the case of the Lac permease, a genetically engineered protease cleavable site in the middle of the permease (*34*) or expression of the functional permease in two fragments (*21*) allowed the analysis of the cross-linked fragments. Similar to MelB (*31*), the native protease cleavable site has been successfully employed here for analysis of intramolecular cross-linking of double-Cys replacements of NhaA.

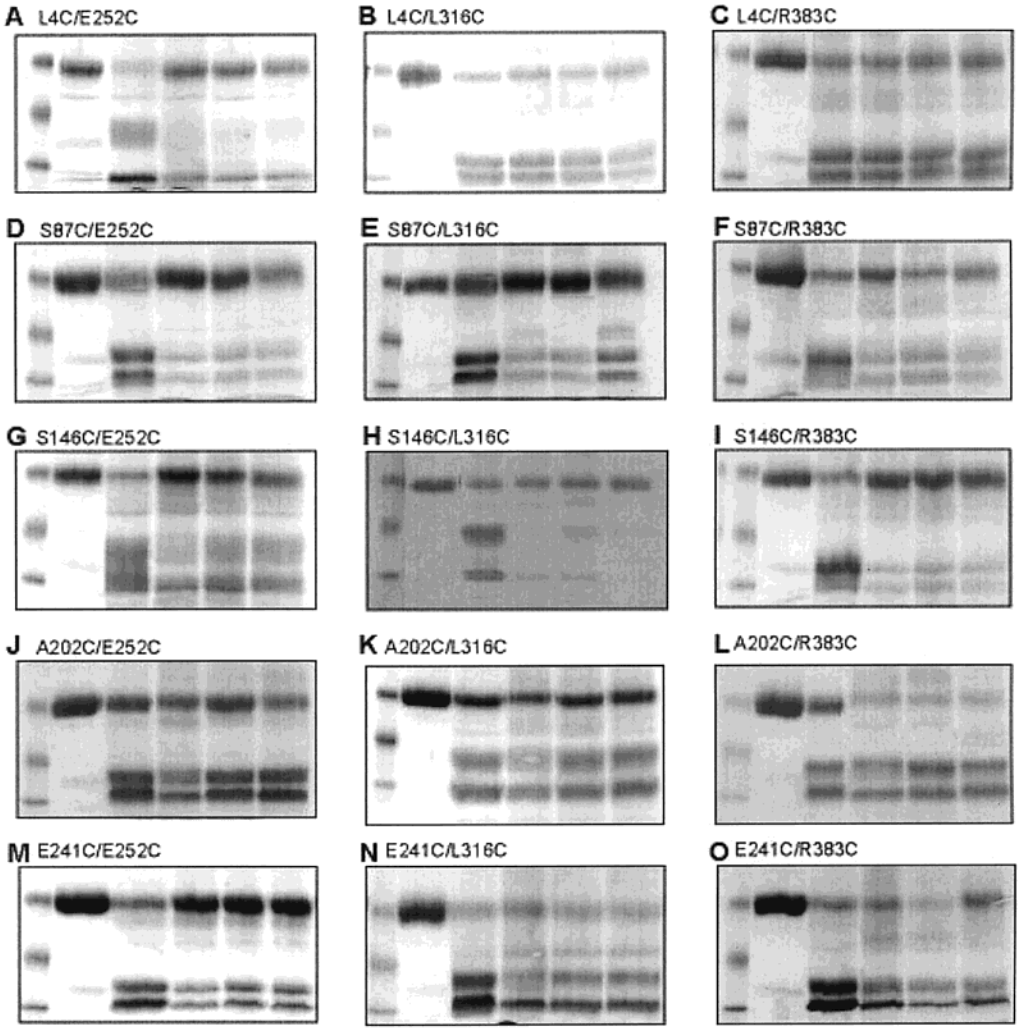

FIGURE 4: In situ cross-linking results between cytoplasmic loops of NhaA. The indicated double-Cys replacement mutants in the cytoplasmic loops of NhaA were treated and presented as described in Figure 3. The results are representative of experiments performed twice or more.

The determination of intra- and intermolecular distances by cross-linking is based on the premise that Cys cross-links are a measure of proximity. However, it should be emphasized that cross-link formation detects dynamic collisions and chemical reactions between residues, not simply their proximities. We therefore conducted the cross-linking reaction in situ on the membranes and not on the purified solubilized protein which requires the presence of detergents. The in situ approach increases the specificity of the cross-linking reaction in several ways: (a) the membrane is the environment in which a membrane protein adopts its native conformation; (b) in the lipid bilayer, the protein motions are restricted and collisions can only occur within the two-dimensional space of the membrane; (c) a strong correlation was found between collision rates in the membrane and proximity (*35*, *36*).

Recently, stochastic dynamic calculations have provided quantitative measures of the length and length dispersions of the widely used molecular cross-linking agents (*32*). The values for the range of S−S distances spanned by the cross-linking reagents *p*-PDM, *o*-PDM, and BMH are 9.2−12.3, 7.7−10.5, and 3.5−15.6 Å, and the average values are 11.13 ± 0.52, 9.39 ± 0.47, and 10.16 ± 2.4 Å, respectively (*32*). The wide S−S distance range of BMH which reflects large span and very high resiliency and overlaps the distances spanned by *o*-PDM and *p*-PDM. Indeed, whenever cross-linking was obtained by *p*-PDM or both *o*-PDM and *p*-PDM, there was cross-linking by BMH (Table 3). However, in several cases where BMH cross-linked, neither *p*-PDM nor *o*-PDM cross-linked (Table 3). In several cases, strong cross-linking was obtained by both *p*-PDM and *o*-PDM albeit *p*-PDM showed somewhat stronger cross-linking in several cases (for example, Figure 3A,D,F). These results are in line with the suggestion that these molecules are not so rigid and the distances spanned by them overlap to a limited extent (*32*). Another possibility that cannot be excluded is that the respective protein loops possess certain mobility. In any event, the cross-linking pattern observed in this study is clearly specific, representing positions in the loops which are in close proximity within NhaA monomer. Thus, none of the Cys replacements used showed any cross-linking between NhaA monomers. Many Cys replacements in the cytoplasmic side, but not periplasmic side, did not exhibit cross-linking by any of the reagents. These results are consistent with the notion that loops are not merely flexible, hydrophilic connections between transmembrane helices that interact randomly.

To obtain a distance map between the respective Cys replacements in the loops of NhaA mutants both at the periplasmic (Figure 5) and at the cytoplasmic (Figure 6) face

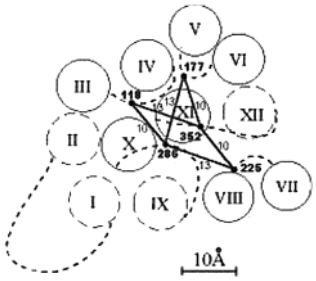

FIGURE 5: Estimated proximities between amino acid residues in the periplasmic loops and schematic representation of the spatial arrangement of TMS in NhaA. Positions of the Cys mutants are indicated as small circles encircling the amino acid residue replaced by Cys. Based on the span distances of the cross-linking reagents [(*32*) and Table 3], the distances in angstroms between the indicated positions are shown. TMS are depicted as large circles with Roman numerals from I to XII. Broken circles designate large uncertainty in the spatial positioning of the respective TMS. Loops are presented as dashed lines in which each dash represents an amino acid.

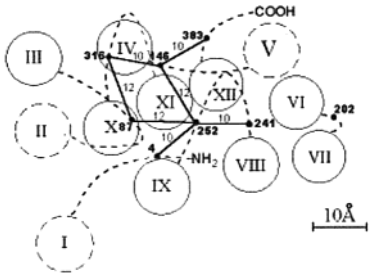

FIGURE 6: Estimated distances between amino acid residues in the cytoplasmic loops and schematic representation of the spatial arrangement of TMS of NhaA. The legend is as in Figure 5.

of NhaA, we used the average S−S distances calculated by Green et al. (*32*) and added the respective standard deviations. The distances may therefore be overestimated with respect to the real ones. We assume that the distances between the Cys replacements are similar to the respective positions in native NhaA.

Given the length of the loops and the possibility that loops are less stable than the transmembrane helices, it is difficult to draw conclusions about helix packing. Nevertheless, our data are most consistent with the views of the periplasmic and cytoplasmic ends of NhaA helices shown in Figures 5 and 6. In these views, the loops are presented as dashed lines in which each dash represents an amino acid. Therefore, there is a correlation between the loop length and the number of amino acids but not the real structure of the loop. The TMS are presented schematically as identical circles spatially positioned in a fashion consistent with the distances measured between the specific positions in the respective loops. Most interestingly, both in the periplasmic and in the cytoplasmic face of NhaA, C-terminal TMS are within close proximity to N-terminal ones. Thus, in the periplasmic side (Figure 5), TMS X is near TMS III and IV, and TMS XI is very near TMS IV. Similarly, in the cytoplasmic side (Figure 6), TMS X faces TMS III, and TMS X, XI, and XII are near TMS IV. TMS IX and VIII are within close proximity to each other, and both are near TMS X, XI, and XII. TMS IX is in close proximity to the N-terminus.

Furthermore, these data have most significant functional implication regarding the pH control of NhaA. We have previously shown that NhaA is controlled by pH which changes its activity over 3 orders of magnitude between pH 7 and 8.5 [reviewed in (*2*) and (*3*)]. We have also shown that the N-terminus of NhaA (*14*) and loop VIII−IX (*13*) undergo a dramatic conformational change with pH which is important for the pH control of NhaA. Strikingly, our cross-linking data reveal (Figure 6) that position 4 of the N-terminus is in close proximity to position 252 of loop VIII−IX. These results highly suggest that in the 3D structure of NhaA the pH-sensitive domains are in close proximity to each other.

Our model predicts that TMS XI is proximal to TMS IV. Very strong support for this contention stems from our previous work. The point mutation G338S of TMS XI alleviates the pH control of NhaA (*11*). Due to overacidification of the cytoplasm, EP432 transformed with plasmidic G338S cannot grow at alkaline pH in the presence of Na^+ (*11*). Suppressor mutations allowing growth of these cells were obtained, and all cluster in TMS IV (*11*, *27*). These results highly suggest a functional interaction between TMS IV and TMS XI. Furthermore, recently we found that all three cross-linking agents, BMH, *p*-PDM, and *o*-PDM, cross-link G338C and D133C (Galili, L., Rimon, A., and Padan, E., unpublished results).

The electron density projection map of NhaA (*17*, *19*) and results from previous biophysical and site-directed mutagenesis studies of NhaA were recently used to construct a detailed three-dimensional molecular model of the protein (*37*). In this study, results from extensive biophysical studies on Lac permease (*38*, *39*), proposing a certain helix packing, as viewed from the periplasmic side, were used as guidelines for helix packing in the NhaA model. Interestingly, this theoretical model also places the C-terminal helices (XI and XII) in close proximity to the N-terminal ones (II and IV).

REFERENCES

1. Padan, E., and Schuldiner, S. (1996) in *Handbook of Biological Physics* (Konings, W. N., Kaback, H. R., and Lolkema, J. S., Eds.) pp 501−531, Elsevier Science, Dordrecht, The Netherlands.
2. Padan, E., and Krulwich, T. (2000) in *Bacterial Stress Responses* (Storz, G., and Hengge-Aronis, R., Eds.) pp 117−130, ASM Press, Washington, DC.
3. Padan, E., Venturi, M., Gerchman, Y., and Dover, N. (2000) *Biochim. Biophys. Acta 1505*, 144−157.
4. Schuldiner, S., and Padan, E. (1996) in *Structure, Function and Molecular Biology of Na/H Exchangers* (Fliegel, L., Ed.) pp 227−249, R. G. Landes Co., Biomedical Publishers, Austin, TX.
5. Padan, E., Maisler, N., Taglicht, D., Karpel, R., and Schuldiner, S. (1989) *J. Biol. Chem. 264*, 20297−20302.
6. Pinner, E., Kotler, Y., Padan, E., and Schuldiner, S. (1993) *J. Biol. Chem. 268*, 1729−1734.
7. Taglicht, D., Padan, E., and Schuldiner, S. (1991) *J. Biol. Chem. 266*, 11289−11294.
8. Taglicht, D., Padan, E., and Schuldiner, S. (1993) *J. Biol. Chem. 268*, 5382−5387.
9. Gerchman, Y., Olami, Y., Rimon, A., Taglicht, D., Schuldiner, S., and Padan, E. (1993) *Proc. Natl. Acad. Sci. U.S.A. 90*, 1212−1216.
10. Rimon, A., Gerchman, Y., Olami, Y., Schuldiner, S., and Padan, E. (1995) *J. Biol. Chem. 270*, 26813−26817.
11. Rimon, A., Gerchman, Y., Kariv, Z., and Padan, E. (1998) *J. Biol. Chem. 273*, 26470−26476.
12. Noumi, T., Inoue, H., Sakurai, T., Tsuchiya, T., and Kanazawa, H. (1997) *J. Biochem. 121*, 661−670.
13. Gerchman, Y., Rimon, A., and Padan, E. (1999) *J. Biol. Chem. 274*, 24617−24624.
14. Venturi, M., Rimon, A., Gerchman, Y., Hunte, C., Padan, E., and Michel, E. (2000) *J. Biol. Chem. 275*, 4734−4742.
15. Rothman, A., Padan, E., and Schuldiner, S. (1996) *J. Biol. Chem. 271*, 32288−32292.

16. Olami, Y., Rimon, A., Gerchman, Y., Rothman, A., and Padan, E. (1997) *J. Biol. Chem. 272*, 1761−1768.
17. Williams, K. A., Kaufer, U. G., Padan, E., Schuldiner, S., and Kühlbrandt, W. (1999) *EMBO J., 18*, 3558−3563.
18. Gerchman, Y., Rimon, A., Venturi, M., and Padan, E. (2001) *Biochemistry 40*, 3403−3412.
19. Williams, K. A. (2000) *Nature 403*, 112−115.
20. Yu, H., Kono, M., McKee, T. D., and Oprian, D. D. (1995) *Biochemistry 34*, 14963−14969.
21. Wu, J., and Kaback, H. R. (1996) *Proc. Natl. Acad. Sci. U.S.A. 93*, 14498−14502.
22. Kaback, H. R., Voss, J., and Wu, J. (1997) *Curr. Opin. Struct. Biol. 7*, 537−542.
23. Davies, B. D., and Mingioli, E. S. (1950) *J. Bacteriol. 60*, 17−28.
24. Ho, S. F., Hunt, H. D., Horton, R. M., Pullen, J. K., and Pease, L. R. (1989) *Gene (Amsterdam) 77*, 51−59.
25. Rosen, B. (1986) *Methods Enzymol. 125*, 328−336.
26. Goldberg, E. B., Arbel, T., Chen, J., Karpel, R., Mackie, G. A., Schuldiner, S., and Padan, E. (1987) *Proc. Natl. Acad. Sci. U.S.A. 84*, 2615−2619.
27. Galili, L., Rothman, A., Kozachkov, L., Rimon, A., and Padan, E. (2002) *Biochemistry 41*, 609−617.
28. Laemmli, U. (1970) *Nature 227*, 680−685.
29. Bradford, W. (1976) *Anal. Biochem. 72*, 248−254.
30. Padan, E., Venturi, M., Michel, H., and Hunte, C. (1998) *FEBS Lett. 441*, 53−58.
31. Ding, P. Z., and Wilson, T. H. (2001) *Biochim. Biophys. Acta 1514*, 230−238.
32. Green, N. S., Reisler, E., and Houk, K. N. (2001) *Protein Sci. 10*, 1293−1304.
33. Kubo, Y., Konishi, S., Kawabe, T., Nada, S., and Yamaguchi, A. (2000) *J. Biol. Chem. 275*, 5270−5274.
34. Sun, J., and Kaback, H. R. (1997) *Biochemistry 36*, 11959−11965.
35. Careaga, C. L., and Falke, J. J. (1992) *J. Mol. Biol. 226*, 1219−1235.
36. Kwaw, I., Sun, J., and Kaback, H. R. (2000) *Biochemistry 39*, 3134−3140.
37. Ravna, A. W., Sylte, I., and Dahl, S. G. (2001) *Receptors Channels 7*, 319−328.
38. Wu, J., and Kaback, H. R. (1997) *J. Mol. Biol. 270*, 285−293.
39. Kaback, H. R., Sahin-Toth, M., and Weinglass, A. B. (2001) *Nat. Rev. Mol. Cell Biol. 2*, 610−622.

BI0261342